Cohesive energy, local magnetic properties, and Curie temperature of Fe_3B studied using the self-consistent LMTO method

Yong Kong* and Fashen Li
Department of Physics, Lanzhou University, Lanzhou 730000, China
(Received 28 January 1997)

The electronic structure of Fe_3B in orthorhombic (o-Fe_3B) and body-centered tetragonal (bct-Fe_3B) structures are calculated using the spin-polarized linear muffin-tin orbitals method. Based upon the calculated electronic structure, we present theoretical results on the cohesive energy (E_{coh}), local magnetic moment (μ_{loc}), and hyperfine magnetic field (H_{hf}) for the two phases of Fe_3B. Effects of the neighboring atoms on μ_{loc} and E_{coh} at individual Fe sites have been discussed in detail. Within the framework of the spin fluctuation of local moments we have evaluated the ratio of the Curie temperature T_C for o- and bct-Fe_3B, and also investigated the volume dependence of T_C. Some numerical results are given and the theoretical results agree qualitatively with the experimental results. [S0163-1829(97)08430-0]

I. INTRODUCTION

The binary iron metalloid compound Fe_3B crystallizes into two phases: the body-centered tetragonal (bct-Fe_3B) and the orthorhombic (o-Fe_3B). In recent years they have been subjected to intense experimental and theoretical studies.[1–4] The great attention to Fe_3B is not only because of the interest given to $Fe_{1-x}B_x$ rapidly quenched crystalline alloys in which metastable Fe_3B have been extensively discussed,[5,6] but also because Fe_3B has the potential for significant applications. Metastable bct-Fe_3B is the main phase in melt-spun permanent magnets with the approximate composition $Nd_4Fe_{78}B_{18}$.[7–9] Due to the low Nd content the material is potentially much cheaper than the $Nd_2Fe_{14}B$ isotropic melt-spun ribbons. In a previous theoretical calculation of the electronic structure for o-Fe_3B by Ching *et al.*[4] using the first-principles orthogonalized linear combinations of atomic orbitals method (OLCAO), the band structure of o-Fe_3B was discussed.

To study systematically the magnetic properties of Fe_3B compounds and to investigate the effect of local environments on the properties of the compounds, we have carried out self-consistent theoretical calculations for bct-Fe_3B and o-Fe_3B. Based upon the results of the spin-polarized calculations for Fe_3B, we study the cohesive energy (E_{coh}) and magnetic properties of Fe_3B in the two structures, and discuss the effects of neighboring atoms on the local magnetic moments (μ_{Fe}) and Fermi contact hyperfine fields (H_{FC}) at the Fe sites when combining the calculated lattice-spacing dependences of μ_{Fe} and H_{FC} for the two phases. Using the Mohn-Wohlfarth approximation within the framework of the spin fluctuation of local moments, we also discuss the Curie temperature T_C of Fe_3B. Our theoretical results should be of value in understanding the electronic and magnetic properties of the $Fe_{1-x}B_x$ alloy, and these results may clarify the magnetic properties of rapidly quenched Nd-Fe-B magnets with low Nd content.

This paper is organized as follows. We will describe the crystal structure of Fe_3B compounds in Sec. II. The linear muffin-tin orbitals (LMTO) method and the calculated techniques are briefly described in Sec. III, and the calculated results on the electronic structure of Fe_3B are also given in this section. In Sec. IV the cohesive energy and the magnetic properties of Fe_3B are further discussed. Volume dependences of μ_{Fe} and H_{FC} at Fe sites in both phases are also presented. Some concluding remarks are included in Sec. V.

II. CRYSTAL STRUCTURE OF Fe_3B

All Fe_3B in two structures are metastable at low temperature and their crystal structures have been completely clarified. The orthorhombic Fe_3B phase is believed to be less stable than the tetragonal phase. The structural information for both phases including lattice constants, type, and number of neighboring atoms are listed in Table I.

o-Fe_3B is isostructural with Fe_3C (cementite),[10] which has an orthorhombic structure with a space group of $V_h^{16}(D_{2h}^{16};Pbnm)$.[11,12] The unit cell contains 4 f.u. and there are two stoichiometrically different Fe sites, $Fe_I(4c)$ and $Fe_{II}(8d)$, and one B site ($4c$) for a total of 16 atoms in the cell. Fe atoms have two B neighbors while a B atom is coordinated by two Fe_I and four Fe_{II}. Fe_I and Fe_{II} have respectively 12 and 11 Fe atoms as neighbors, and the Fe_{II}-Fe distances are slightly smaller than the Fe_I-Fe distances.

bct-Fe_3B has a body-centered-tetragonal lattice with a space group of $S_4^2(I\bar{4})$[1,13] and 8 f.u. per cell. The structure can be considered as rather close packed, resulting in high coordination numbers. Iron atoms in three sets of eightfold positions are assigned to three different Fe sites: Fe_I, Fe_{II}, and Fe_{III}. Fe_I has 12 iron neighbors but Fe_{II} and Fe_{III} have 10 iron neighbors, respectively. They are coordinated by 2, 4, and 3 B atoms in turn. The B atoms in one eightfold position have 9 iron neighbors which form a capped triangular prism.

III. COMPUTATIONAL PARAMETERS AND CALCULATED RESULTS

Using the LMTO method that was described and reviewed in Refs. 14 and 15, we here perform a semirelativistic

TABLE I. Crystal structure information of Fe_3B compounds.

	o-Fe_3B			bct-Fe_3B			
Structure	Orthorhombic			Body-centered tetragonal			
Lattice cons.	$a=0.4454$			$a=0.8630$			
(nm)	$b=0.5433$						
	$c=0.6656$			$c=0.4290$			
Z (mol/cell)	4			8			
Space group	$Pbnm(V_h^{16})$			$I\bar{4}\ S_4^2$			
Sites	Fe_I	Fe_{II}	B	Fe_I	Fe_{II}	Fe_{III}	B
Neighbor atoms	$2Fe_I$,$10Fe_{II}$ 2B	$5Fe_I$,$6Fe_{II}$ 2B	$2Fe_I$,$4Fe_{II}$	$5Fe_I$,$2Fe_{II}$ $5Fe_{III}$,2B	$2Fe_I$,$5Fe_{II}$ $3Fe_{III}$,4B	$5Fe_I$,$3Fe_{II}$ $2Fe_{III}$,3B	$2Fe_I$,$4Fe_{II}$ $3Fe_{III}$

spin-polarized band calculation on the two phases of iron metalloid compound Fe_3B: o- and bct-Fe_3B. For the merits and disadvantages of the method, as well as the technique details, refer to Refs. 14 and 15. In our calculation, the exchange-correlation term is taken as the form deduced by von Barth and Hedin.[16] The Brillouin-zone integration is carried out for $64\vec{k}$ and $75\vec{k}$ points in the irreducible zone of bct- and o-Fe_3B, respectively. We use partial waves up to $l=2$ for the valence electrons of Fe, which are $3d,4s$ electrons, and apply s,p orbitals for the $2s,2p$ electrons of B. The convergence is assumed when the root-mean-square error of the self-consistent potential is smaller than 1 mRy.

In the atomic-sphere approximation (ASA) the atomic radius assigned to the atomic sites should be chosen so as to satisfy $V=(4\pi/3)\Sigma_i Q_i S_i^3$, where V is the volume of unit cell, and S_i is the atomic radius of the equivalent Q_i atoms in the cell. Here we take the same radius for iron atoms located at different sites in the cell. For both structures of Fe_3B we take the same ratio of radius $p=S_B/S_{Fe}=0.75$ which is approximately equal to the ratio of the covalent radius between boron and iron atoms, so the values of S_{Fe} and S_B are automatically defined by the above equation in accordance with the cell volume.

The calculations are also performed for the two phases of Fe_3B with various unit cell volumes, so that one can investigate the volume dependences of magnetic properties for Fe_3B. Moreover, here we would like to point out that, since the calculated results are sensitive to the chosen atomic radius and affected by the choice of the exchange-correlation potentials, it is inevitable that there are some quantitative errors when we compare the calculated results with the experimental results. Nevertheless, the qualitative agreement with experimental results is meaningful.

The spin-projected density of states (DOS) curve for each site in both Fe_3B are shown in Fig. 1. As can be seen, d states dominate the DOS of Fe atoms and peak shapes for different iron sites in the same Fe_3B are very similar. In both Fe_3B the Fermi level lies nearly above the spin-up d DOS but falls actually in d DOS. Thus the occupation number $n_d^{\uparrow}$ of electrons in the spin-up d subband is more than that in the spin-down d subband, and the d states for both spin directions contribute to the DOS at Fermi level, $N(E_F)$. The hybridized s states between Fe and B form a discretized structure in the lowest-energy region. Certainly there are different features between the DOS of the two Fe_3B. The d DOS at Fe sites in the two structures have indicated great difference. Most d DOS of Fe in bct-Fe_3B construct two peaks but those in o-Fe_3B form a continuous region. In Table II we have listed some electronic structure parameters calculated on the two structures of Fe_3B. It can be seen that in both Fe_3B the average occupation $\overline{n_d}$ of d electrons is the same, although the occupation number n_d at different Fe sites is quite different.

IV. DISCUSSIONS

A. Cohesive energy

It is well known that the cohesive properties of transition-metal compounds are closely related to their electronic structure. The cohesive properties of $3d$ transition metal carbides

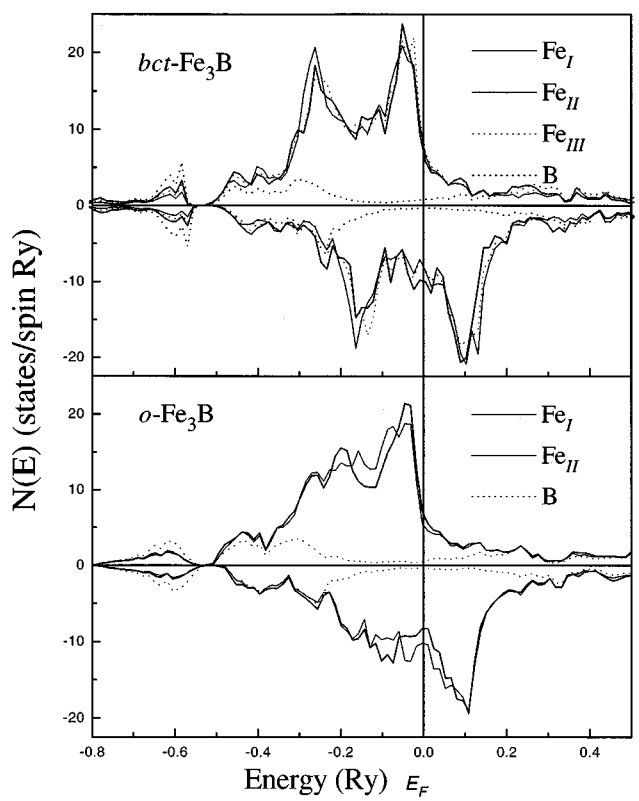

FIG. 1. The calculated spin-polarized local DOS at individual sites for both structures of Fe_3B.

TABLE II. Calculated electronic structure parameters for Fe_3B compounds. Here n and n_l denote total and l occupation number at a site, respectively. $N(E_F)$ is DOS at the Fermi level (in units of states/spin Ry) and E_{total} represents the total energy of the system (in units of Ry).

	o-Fe_3B			bct-Fe_3B			
	Fe_I	Fe_{II}	B	Fe_I	Fe_{II}	Fe_{III}	B
$n_s^\uparrow$	0.311	0.312	0.404	0.309	0.313	0.317	0.428
$n_p^\uparrow$	0.421	0.439	0.748	0.413	0.456	0.448	0.690
$n_d^\uparrow$	4.369	4.300		4.396	4.318	4.324	
$n^\uparrow$	5.101	5.051	1.152	5.119	5.087	5.089	1.118
$n_s^\downarrow$	0.316	0.318	0.423	0.317	0.315	0.324	0.451
$n_p^\downarrow$	0.453	0.474	0.861	0.454	0.482	0.490	0.816
$n_d^\downarrow$	2.276	2.367		2.206	2.401	2.330	
$n^\downarrow$	3.045	3.158	1.284	2.977	3.198	3.144	1.267
$n^\uparrow+n^\downarrow$	8.146	8.209	2.436	8.096	8.285	8.233	2.385
$n^\uparrow-n^\downarrow$	2.056	1.893	−0.132	2.142	1.889	1.945	−0.149
$N(E_F)^\uparrow$	5.209	6.666	0.541	7.796	6.849	8.378	0.816
$N(E_F)^\downarrow$	10.274	8.313	0.357	8.145	9.937	8.082	0.326
$N(E_F)$	15.483	14.979	0.898	15.941	16.786	16.460	1.142
E_{total}		−30690.689			−30690.228		

have been studied both experimentally and theoretically[17] and *ab initio* results in carbides and nitrides with NaCl-type structure are also reported.[18] However, no such results are available for the borides. It is therefore of considerable interest to calculate the cohesive energies of the more complex transition-metal borides. Basing upon the calculated total energy E_{total} for Fe_3B, we can estimate the cohesive energy E_{coh} of Fe_3B compounds.

The average cohesive energy per atom for the two phases of Fe_3B can be defined by

$$E_{coh}=-\left(\frac{1}{16}\right)\left(E_{total}-\sum E_A\right),$$

where the total atomic energies E_A are to be summed over all 16 atoms of the cell. From the LMTO calculations we have found a total energy of $E_{total}=-30690.689$ Ry and -30690.228 Ry for o- and bct-Fe_3B, respectively. Using the atomic energies calculated by Häglund *et al.*,[18] $E_{Fe}=-2540.787$ Ry and $E_B=-48.537$ Ry, we obtain $E_{coh}=444$ mRy/atom$=5.82\times10^5$ J/mol for o-Fe_3B and $E_{coh}=415$ mRy/atom$=5.44\times10^5$ J/mol for bct-Fe_3B. It can be seen that the estimated value of E_{coh} for o-Fe_3B is slightly larger than that for bct-Fe_3B, which is perhaps connected with the lower occupation energy of electrons in o-Fe_3B. Unfortunately, no experimental results in E_{coh} for Fe_3B are available to compare our evaluated E_{coh}, but the *ab initio* results on carbides and nitrides[18] have shown that the shift between theoretical and experimental energies is nearly remarkably constant and the theoretical values can be successfully used to study both general trends and details in the variation of E_{coh}. Thus it will be interesting to compare our result for the E_{coh} of Fe_3B with results from future investigations of 3d transition-metal borides.

B. Local magnetic moment and hyperfine field

We have listed the calculated results on μ_{Fe} at Fe atoms for Fe_3B in both structures in Table III. Since Fe_3B are metastable, no available experimental results in μ_{Fe} for Fe $_3$B can be used to compare our calculated μ_{Fe}, but it can be seen that, for o-Fe_3B, the calculated average magnetic mo-

TABLE III. Calculated μ_{Fe} (in μ_B), H_{FC} (in T) and its valence contribution $H_{FC,val}$ and the coupling constants A and B (in T/μ_B) for Fe_3B. And experimental results on $\overline{\mu_{Fe}}$ (Ref. 10) and H_{hf} (Refs. 1 and 20).

	o-Fe_3B			bct-Fe_3B			
	Fe_I	Fe_{II}	Average	Fe_I	Fe_{II}	Fe_{III}	Average
μ_{Fe}	2.06	1.89	1.95	2.14	1.89	1.95	1.99
μ (Expt.)			2.0				
H_{FC}	−26.8	−25.4	−25.9	−29.2	−23.0	−27.0	−26.4
$H_{FC,val}$	−1.72	−2.14	−2.01	−3.27	0.20	−3.11	−2.06
H_{hf} (Expt.)	26.4	23.5	24.5	28.7	22.5	26.7	26.0
	±0.5	±0.5	±0.5	±0.2	±0.2	±0.3	±0.3
A	−12.18	−12.33		−12.11	−12.28	−12.26	
B	−0.90	−1.09		−1.62	0.10	−1.53	

ment $\overline{\mu_{Fe}}$ agrees well with the extrapolated value (listed in Table III) from $Fe_3C_{1-x}B_x$ at 4.2 K,[10] and the calculated μ_{Fe} at individual Fe sites are also consistent with the results obtained by Ching *et al.*[4]

One of the characteristic quantities of spin-polarized electronic structure is that the local magnetic moment μ_{loc} of an atom in the material depends closely upon the neighboring environment of the atom, i.e., the type and the number of neighbors, and the interatomic distances with neighbors. Ching *et al.*[4] have concluded that the μ_{Fe} is reduced by increasing the boron concentration. The calculated results for bct-Fe_3B have shown that there is a great difference among the μ_{Fe} at three sites. The μ_{Fe} at Fe_I ($2.14\mu_B$) is much larger than that at Fe_{II} ($1.89\mu_B$), and the μ_{Fe} at Fe_{III} is intermediate. Since the Fe neighbors of the Fe atom at three sites are very similar, the difference of μ_{Fe} is mainly determined by the effect of the neighboring boron. Fe_I has only two boron neighbors while Fe_{II} has four boron atoms as neighbors; it is suggested that the bonding interactions between Fe and B promote the itinerancy of Fe 3*d* electrons and decrease the exchange splitting: the more boron neighbors of the Fe atom, the smaller the μ_{Fe} of the Fe atom. On the contrary, in *o*-Fe_3B the Fe atoms at both sites all have two boron atoms as neighbors and the Fe-B distances are close, thus the effects of boron atoms on the μ_{Fe} seem to be alike and do not lead to such a large difference of μ_{Fe} as that in bct-Fe_3B. So the smaller μ_{Fe} at Fe_{II} than that at Fe_I can only be assigned to the influence of the neighboring Fe atoms. Analyzing the Fe-Fe distance, we can find that there are smaller interatomic distances between Fe_{II} and its Fe neighbors when compared to those between Fe_I and its Fe neighbors. It seems that the stronger hybridized interactions between Fe_{II} and its Fe neighbors due to smaller Fe_{II}-Fe distances decrease the exchange splitting of $Fe_{II}3d$ electrons and result in a smaller μ_{Fe} at Fe_{II}.

We have illustrated the dependences of the μ_{Fe} at Fe sites and the $\overline{\mu_{Fe}}$ in bct- and *o*-Fe_3B on the volume of the unit cell in Fig. 2(a). It has been shown that the μ_{Fe} at each Fe site in both Fe_3B decrease greatly with the reduction of the unit cell volume. Using the formula $\mu_{loc}=A+B\ln V$, we can fit the changes of the $\overline{\mu_{Fe}}$ for both Fe_3B approximately and obtain the volume dependence of the $\overline{\mu_{Fe}}$ from the slope of the fitting curve, $d\overline{\mu_{Fe}}/d\ln V=5.11\mu_B$ and $3.71\mu_B$ for bct- and *o*-Fe_3B, respectively. The decrease of μ_{Fe} in bct-Fe_3B with the unit cell compression is much larger than that in *o*-Fe_3B. Moreover, it is interesting to notice that in bct-Fe_3B the decrease of μ_{Fe} at Fe_{II} with the reduction of the unit cell volume is much smaller than those at other sites. Since Fe_{II} has the most B neighbors, it is indicated that the strong shielding effect of B neighbors has partly cancelled the effect of volume compression on μ_{Fe} and makes the μ_{Fe} at Fe_{II} relatively stable against the compression of the lattice.

The main contribution to the hyperfine magnetic field H_{hf} of the atom is in the 3*d* transition metal compound H_{FC} of an atom and can be decomposed into $H_{FC,core}$ and $H_{FC,val}$. The former is the core contribution, which comes from the polarization of the core atoms, and the latter is the contribution of conducted electron polarization, which is

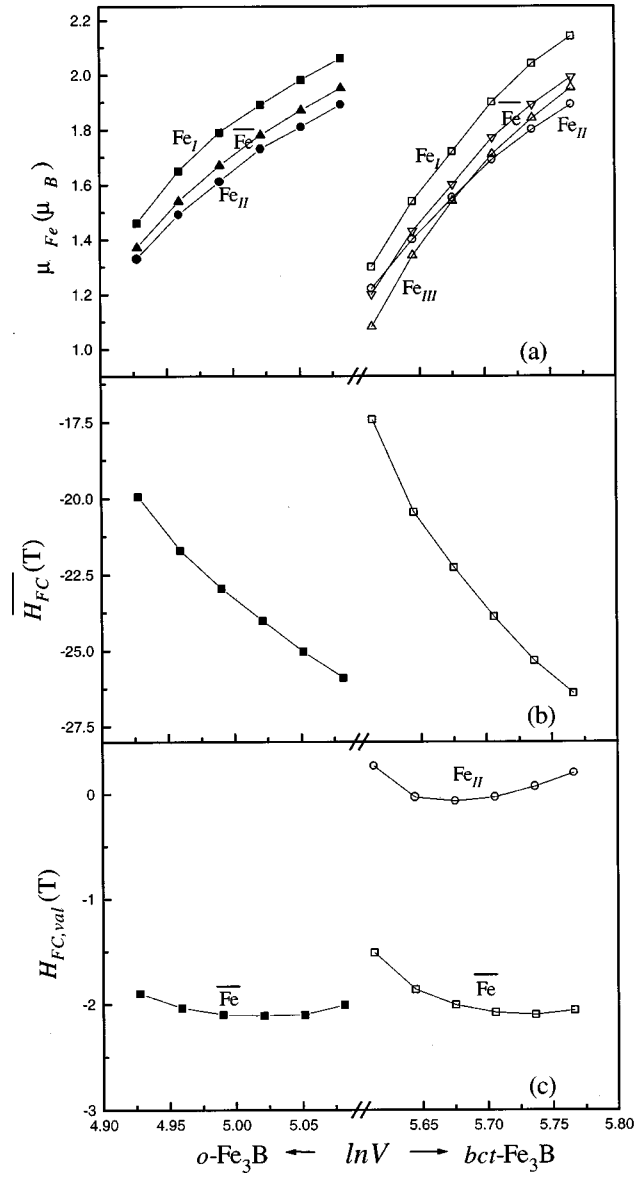

FIG. 2. The unit cell volume dependence of μ_{Fe}, H_{FC}, and its valence contribution $H_{FC,val}$ in Fe_3B. The solid and hollow symbols represent those in *o*- and bct-Fe_3B, respectively.

mainly produced by the *sd* hybridization between the *s* orbitals of the atom and the *d* orbitals of its neighbors. In Table III we have also listed the calculated H_{FC} of Fe and its valence contribution $H_{FC,val}$ for both Fe_3B. Here H_{FC} are calculated according to the prescription given by Akai *et al.*[19] It is found that the calculated H_{FC} at Fe in both Fe_3B are slightly larger than the experimental results[1,20] at room temperature listed in the table. Since H_{hf} decreases with increasing temperature, our results in H_{FC} are in excellent agreement with the experimental results. Like most transition metal compounds the $H_{FC,val}$ at Fe sites in both Fe_3B are only a minor contribution to H_{FC}. In *o*-Fe_3B the $H_{FC,val}$ at the Fe_{II} site takes a larger portion in the H_{FC} than that at an Fe_I site. It is the reason that the Fe_{II}-Fe interaction is stronger than that between Fe_I and Fe due to the shorter Fe_{II}-Fe distances, while in bct-Fe_3B the strong shielding effect of four B neighbors surrounding an Fe_{II} site results in a small positive $H_{FC,val}$ at the Fe_{II} site, which differs greatly from

those at the Fe_I and Fe_{III} sites. Generally $H_{FC,core}$ is proportional to μ_{loc} of an atom and $H_{FC,val}$ is related to the average magnetic moments μ_N of its neighbors. So the H_{FC} at an Fe site can be phenomenologically expressed as follows:[19,21]

$$H_{FC}=H_{FC,core}+H_{FC,val}=A\mu_{Fe}+B\overline{\mu_N},$$

where A and B are defined as hyperfine coupling constants. Using the calculated μ_{Fe}, we have evaluated the coupling constants A and B and listed them in Table III, also. It has been found that in both Fe_3B there are similar coupling coefficients A but greatly different coefficients B. In o-Fe_3B a larger coefficient B at Fe_{II} has indicated a stronger Fe_{II}-Fe interaction while in bct-Fe_3B a positive B at Fe_{II} has revealed the shielding effect of boron atoms which has changed the Fe_{II}-Fe interactions and reversed the polarization direction of the sd hybridization between Fe_{II} and Fe.

The average H_{FC} and the average $H_{FC,val}$ at Fe sites in both Fe_3B are given in Figs. 2(b) and 2(c), in which the solid symbols represent the $\overline{H_{FC}}$ and the $\overline{H_{FC,val}}$ in o-Fe_3B while the hollow symbols describe those in bct-Fe_3B. Assuming a linear relation between the $\overline{H_{FC}}$ and the logarithmic volume of the unit cell, we find that the value of $\overline{H_{FC}}$ at Fe sites decreases with the compression of the unit cell by $d|\overline{H_{FC}}|/d\ln V=$ 37.93 and 56.94 T for o- and bct-Fe_3B, respectively. The H_{FC} at Fe sites in o-Fe_3B is more stable than that in bct-Fe_3B against the compression of the unit cell volume. In both Fe_3B the changes of the $\overline{H_{FC,val}}$ at Fe sites with the logarithmic volume are not monotonous and indicate the complexity of the volume dependence of the Fe-Fe interactions in Fe_3B. Especially, we show the $H_{FC,val}$ at an Fe_{II} site in bct-Fe_3B under various unit cell volumes in Fig. 2(c), also. It is interesting to observe that the $H_{FC,val}$ of the Fe_{II} atom in bct-Fe_3B changes not only its amplitude but also its sign, which implies that the compression of the unit cell volume changes not only the strength of Fe_{II}-Fe interactions but also the polarized direction of the sd hybridization between them.

C. Curie temperature

Curie temperature T_C is the important characteristic temperature of the metallic ferromagnetic materials and its pressure (volume) dependence is a property of unusual physical interest. Experimentally, Fruchart *et al.*[10] have extracted the T_C (897 K) of the o-Fe_3B by extrapolating the T_C of $Fe_3C_{1-x}B_x$, and the T_C (786 ± 3 K) of bct-Fe_3B (Ref. 7) has also been determined, although both Fe_3B are metastable. According to the calculated results of electronic structure, we can use the Mohn-Wohlfarth approximation[22] to discuss the T_C of Fe_3B and their volume dependence within the framework of the spin fluctuations of local magnetic moment. In Mohn-Wohlfarth theory T_C is determined by the solution of the equation

$$T_C^2/T_S^2+T_C/T_{sf}-1=0,$$

where T_S is the Stoner-model Curie temperature, and T_{sf} is a characteristic temperature describing the influence of spin fluctuations and given by

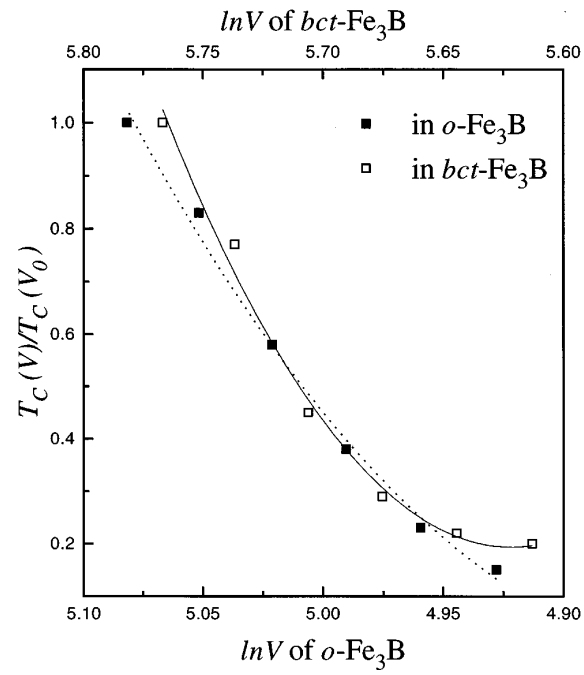

FIG. 3. The volume dependence of the T_C for Fe_3B.

$$T_{sf}=(M_0^2/40k_B)[1/N_\uparrow(E_F)+1/N_\downarrow(E_F)-2I],$$

where M_0 is the zero-temperature magnetic moment, k_B is the Boltzmann's constant, $N_\uparrow(E_F)$ and $N_\downarrow(E_F)$ are the up- and down-spin DOS at E_F, and I is the Stoner parameter. The quantities $M_0, N_\uparrow(E_F)$, and $N_\downarrow(E_F)$ are directly determined by theoretical electronic structure. The Stoner parameter I for transition metals and their compounds may be written as[23]

$$I=\sum_t I_t[N_t(E_F)/N(E_F)]^2,$$

where I_t and $N_t(E_F)$ are the Stoner parameter and the DOS for the atom at site t. For I_t we have used the values from the work of Janak.[24]

It is worthwhile noting that Woods *et al.*[25] are already successful in predicting the relative change of T_C in iron-based rare-earth compounds with applying the Mohn-Wohlfarth theory, although the absolute T_C of strong ferromagnets cannot be correctly determined by this model.[26] In our discussion, we do not directly evaluate the absolute T_C of Fe_3B with this model but work out the ratio $T_C(V)/T_C(V_0)$ with the compression of the unit cell volume. Using this model, we have first evaluated the ratio T_C^{bct}/T_C^o between the T_C for both Fe_3B to be 0.83, which agrees well with the experimental result 0.88. It is also suggested that the prediction of the volume dependence of the T_C for Fe_3B with this model will be qualitatively correct. We have plotted the evaluated $T_C(V)/T_C(V_0)$ for both Fe_3B with the volume compression in Fig. 3 and fitted them well with the second order polynomial of the logarithmic unit cell volume. From the fitted curve a critical volume V_c corresponding to the disappearing point of ferromagnetism can be evaluated to be $0.85V_0$ for o-Fe_3B but cannot be found for bct-Fe_3B. Moreover, from the obvious linear relation between $dT_C/d\ln V$

and lnV, we have derived the volume dependence of T_C for both o- and bct-Fe_3B as approximately $(1+CT_C)^{1/2}$, where C is a constant.

V. CONCLUSIONS

We have performed self-consistent spin-polarized electronic structure calculations on the ferromagnetic Fe_3B crystallizing in orthorhombic and body-centered-tetragonal structures using the LMTO methods. The theoretical results on μ_{Fe} and H_{FC} agree well with experimental measurements. According to the calculated results, the effects of neighboring atoms on μ_{Fe} and H_{FC} at individual Fe sites have been discussed in detail. Using the Mohn-Wohlfarth theory we have discussed the volume dependence of the Curie temperature T_C for o- and bct-Fe_3B. In summary some concluding remarks are presented as follows.

(1) The cohesive energy per atom in cell E_{coh} has been evaluated from the calculated electrons total energy. The evaluated E_{coh} for o-Fe_3B is slightly larger than that for bct-Fe_3B.

(2) The local magnetic moment and hyperfine field of an Fe atom are related closely to the neighboring environments of the Fe atom. The B neighbors surrounding an Fe atom decrease the exchange splitting at the Fe site and then reduce the magnetic moment of the Fe atom. The more B neighbors surrounding an Fe atom, the smaller the magnetic moment of the Fe atom. The larger Fe-Fe distances produce a larger Fe magnetic moment but a smaller valence contribution to H_{FC}.

(3) The shielding effect from B atoms makes μ_{Fe} at an Fe_{II} in bct-Fe_3B much more stable against the volume compression. It also changes the Fe_{II}-Fe interactions and leads to a small positive $H_{FC,val}$ at the Fe_{II} site.

(4) According to our calculated results, the ferromagnetism of o-Fe_3B will disappear when the compression of the unit cell volume is larger than 15%. For two structures of Fe_3B the derived volume dependences of the T_C all follow $(1+CT_C)^{1/2}$, where C is a constant.

Since the Fe_3B in both structures are not stable phases, there are not enough experimental results to be compared with our calculated results. We expect to compare completely our calculated results with experimental measurements from future investigations of Fe_3B.

ACKNOWLEDGMENTS

The calculations were carried out on a DEC-3000 workstation. This project was supported by the Natural Science Foundation of China and by the Doctoral Research Fund of National Education Committee of China.

*Present address: Fakultät für Physik und Astronomie, Institut für Experimentalphysik III, AG Festkörperspektroskopie, Ruhr-Universität Bochum, D-44801 Bochum, Germany. Electronic address: kong@ep3.ruhr-uni-bochum.de

[1] G. Le Caer and J. M. Dubois, Phys. Status Solidi A **64**, 275 (1981).
[2] W. Coene, F. Hakkens, R. Coehoorn, D. B. de Mooij, C. de Waard, J. Fidler, and R. Grössinger, J. Magn. Magn. Mater. **96**, 189 (1991).
[3] S. M. Cheremisin, A. Yu. Dudkin, and I. V. Matveev, Nucl. Instrum. Methods Phys. Res. B **84**, 102 (1994).
[4] W. Y. Ching, Y. N. Xu, B. N. Harman, Jun Ye, and T. C. Leung, Phys. Rev. B **42**, 4460 (1990).
[5] M. B. Fernandez van Raap and F. H. Sanchez, J. Appl. Phys. **66**, 875 (1989).
[6] F. H. Sanchez, Y. D. Zhang, J. I. Budnick, and R. Hasegawa, J. Appl. Phys. **66**, 1671 (1989); Y. D. Zhang, J. I. Budnick, J. C. Ford, W. A. Hines, and F. H. Sanchez, *ibid.* **61**, 3231 (1987).
[7] R. Coehoorn, D. B. de Mooij, and C. de Waard, J. Magn. Magn. Mater. **80**, 101 (1989).
[8] R. Coehoorn, D. B. de Mooij, J. P. W. B. Duchateau, and K. H. J. Buschow, J. Phys. (France) Colloq. **49**, C8-669 (1988).
[9] R. Coehoorn and C. de Waard, J. Magn. Magn. Mater. **83**, 228 (1990).
[10] D. Fruchart, P. Chaudouet, R. Fruchart, A. Rouault, and J. P. Senateur, J. Solid State Chem. **54**, 246 (1984).
[11] E. J. Fasiska and G. A. Jeffrey, Acta Crystallogr. **19**, 463 (1965).
[12] R. W. G. Wyckoff, *Crystal Structures* (Interscience, New York, 1965).
[13] B. Aronsson, Acta Chem. Scand. **9**, 137 (1955).
[14] O. K. Anderson, Phys. Rev. B **12**, 3050 (1975).
[15] H. L. Skriver, in *The LMTO Method*, edited by M. Cardona, P. Fulde, and H. J. Queisser (Springer, Berlin, 1984).
[16] U. Von Barth and L. Hedin, J. Phys. C **5**, 1629 (1972).
[17] A. Fernandez Guillermet and G. Grimvall, J. Phys. Chem. Solids **53**, 105 (1992).
[18] J. Häglund, G. Grimvall, T. Jarlborg, and A. Fernandez Guillermet, Phys. Rev. B **43**, 14 400 (1991).
[19] H. Akai, M. Akai, S. Blügel, B. Drittler, H. Ebert, K. Terakura, R. Zeller, and P. H. Dederichs, Prog. Theor. Phys. Suppl. **101**, 11 (1990).
[20] W. K. Choo and R. Kaplow, Metall. Trans. A **8**, 417 (1977).
[21] Z. M. Stadnik and G. Stronik, Hyperfine Interact. **47**, 275 (1989).
[22] P. Mohn and E. P. Wohlfarth, J. Phys. F **17**, 2421 (1987).
[23] S. S. Jaswal, Solid State Commun. **52**, 127 (1984).
[24] J. F. Janak, Phys. Rev. B **16**, 255 (1977).
[25] J. P. Woods, B. M. Patterson, A. S. Fernando, S. S. Jaswal, D. Welipitiya, and D. J. Sellmyer, Phys. Rev. B **51**, 1064 (1995).
[26] Q. N. Qi, R. Skomski, and J. M. D. Coey, J. Phys. Condens. Matter **6**, 3245 (1994).